Extraction, Isolation, and Characterization of Nanocrystalline Cellulose from *Barangan* Banana (*Musa acuminata* L.) Peduncles Waste

Ratna Ratna[1,2], Nasrul Arahman[1,3,4,5,6], Agus Arip Munawar[2], and Sri Aprilia[1,3*]

[1]*Doctoral Program, School of Engineering, Post Graduate Program, Universitas Syiah Kuala, Darussalam, Banda Aceh 23111, Indonesia*

[2]*Department of Agricultural Engineering, Universitas Syiah Kuala, Darussalam, Banda Aceh 23111, Indonesia*

[3]*Department of Chemical Engineering, Universitas Syiah Kuala, Darussalam, Banda Aceh 23111, Indonesia*

[4]*Graduate School of Environmental Management, Universitas Syiah Kuala, Darussalam, Banda Aceh 23111, Indonesia*

[5]*Research Center for Environmental and Natural Resources, Universitas Syiah Kuala, Jl. Hamzah Fansuri No. 4, Darussalam, Banda Aceh 23111, Indonesia*

[6]*Atsiri Research Center, Universitas Syiah Kuala, Jl. Syeh A. Rauf, Darussalam, Banda Aceh 23111, Indonesia*

* ***Corresponding author:***

email: sriaprilia@unsyiah.ac.id

Received: May 18, 2022
Accepted: October 3, 2022

DOI: 10.22146/ijc.74718

Abstract: *Microwave-assisted acid hydrolysis has an impact on the characteristics of nanocrystalline cellulose (NCCs). In this study, NCCs was prepared from banana peduncles through hydrolysis of sulfuric acid (concentrations of 1, 2, and 3 M) and hydrolysis time (0.5 and 1.5 h) assisted by microwave and ultrasonic energy to obtain the best NCCs. The characterization of NCCs properties, namely, yield, morphology, functional groups, crystallinity, heat resistance, particle size, and color. The results showed that the yield of NCCs decreased as sulfuric acid concentration and the time length of hydrolysis increased. The FTIR spectra of NCCs showed the most relevant molecular bands, namely O–H, C–H, and C–O, at the wavenumbers range of 3200–4000, 2500–3200, and 500–1500 cm^{-1}, respectively. The TGA test showed that the decomposition of NCCs occurred at a temperature of 275.35–409.40 °C, with a weight loss ranging from 84.00% to 94.09%. Crystallinity index and crystal sizes range from 53.99% to 57.33% and 22.35 to 36.28 nm, respectively. The brightest color of NCCs powder was generated with 1 M sulfuric acid and a hydrolysis time of 0.5 h. In conclusion,* barangan *banana peduncles waste can be used as raw material for producing NCCs.*

Keywords: *nanocrystalline cellulose;* barangan *banana peduncles waste; acid hydrolysis; microwave; ultrasonic*

■ INTRODUCTION

Globally, people grow around 5.6 million hectares of bananas, with a production rate of 120 million tons annually. The banana industry is estimated to generate a turnover of 8 billion USD per year [1]. One sector using the most bananas is the food industry [2]. The abundance use of bananas leads to banana waste, including bark, pseudostem, leaves, rejected bananas, peduncles, and fiber [3]. Each banana tree produces one peduncle of bananas, and the tree will become waste after harvesting. It is estimated that every hectare of banana plantations produces nearly 220 tons of biomass waste [4]. The unused by-product of banana processing is banana peduncles. This by-product is promising because it contains lignocellulose to produce cellulose [5].

Cellulose is widely used as a polymer matrix and has grown rapidly in the last decade [6] because of its advantages, such as being non-toxic, low density, good mechanical properties, environmentally friendly, inexpensive, and biodegradable [7-8]. Cellulose has a linear chain structure of a hydro-glucose monomer unit-

linked via 1-4 β, with amorphous and crystalline regions. The structures, properties, and sizes of cellulose depend on the sources [9]. Cellulose is the largest proportion of lignocellulosic substances; from a structural perspective, cellulose is a polymer formed by β-D glucose units ($C_6H_{12}O_6$) [10-12].

Nanocrystalline cellulose (NCCs) are prominent cellulose derivatives because of their exclusive features and outstanding mechanical properties, high aspect ratio to diameter, several micrometers length, high surface reactivity, and low density [12]. Structurally, NCCs are basic needle-shaped crystals with intact crystal features. NCCs are generally 5–10 nm wide and 500–1000 nm long [13-14]. NCCs are highly crystalline nanocrystals that can be produced from cellulose substances by acids [15-17]. NCCs produced from empty peduncles were previously modified by tannic acid and decyl amine [9]. NCCs have also been successfully extracted from seaweed [18], corn cobs [19-20], oil palm empty fruit peduncles [21-22], ramie fiber [23], waste paper [24], bagasse [25], and kenaf [26].

Cellulose hydrolysis in acid can be done by strong and weak acids at high temperatures and pressures, and by concentrated acid at low temperatures and pressures [27-28]. NCCs can be obtained from various sources using several alkalines or acid hydrolysis [29-30]. The functional properties of substances can be improved by modifying chemical or physical processes, such as acid hydrolysis, oxidation, ultrasonication, and microwave [31]. Microwave energy has been found as an alternative to heating in acid or alkali treatment [32]. Recently, microwave-assisted alkali treatment and microwave-assisted acid hydrolysis before ultrasonication were used to generate higher yields of NCCs [33]. Microwave irradiation can increase the yield of compounds drastically in a short time [34-35]. Mechanical treatment, such as sonication, spreads a stable and uniform suspension of NCCs [36]. Sonication is an alternative for degradation [37] in producing NCCs.

Nanocellulose can be produced from various wastes from agricultural crops [38]. Mocktar et al. has produced nano-cellulose from the kenaf core (*Hibiscus cannabinus*) by chemical method [26]. Produced nanocrystalline cellulose from eucalyptus was hydrolyzed using sulfuric acid by conventional methods and assisted by thermostable. The nanocrystalline cellulose produced by the thermostable method showed much better thermal stability than hydrolyzed by the conventional method [39]. Kusmono et al. have produced nanocrystalline cellulose made from flax fiber by hydrolysis of sulfuric acid using a conventional method with a hot plate [23]. Rahmawati et al. reported that nanocrystalline cellulose was isolated from *Typha* sp. through conventional acid hydrolysis using a hot plate with a reflux system [40]. There have been many reports on the hydrolysis of nanocrystalline cellulose from plant fibers and agricultural wastes. However, there has been no report on the hydrolysis method and characterization of NCCs from the waste of *barangan* banana (*Musa acuminata* L.) peduncles. Therefore, this study examines the production of NCCs from the waste of *barangan* banana peduncles by studying the alkalizing, bleaching, and hydrolysis treatment of sulfuric acid with variable concentrations of sulfuric acid and hydrolysis time using microwaves-ultrasonics energy on the properties and characteristics of NCCs. The analysis covered the yield and characterization of NCCs properties, namely, morphology, functional groups, crystallinity, heat resistance, particle size, and color.

■ EXPERIMENTAL SECTION

Materials

The waste of *barangan* banana (*Musa acuminata* L.) peduncles was taken from the community around Banda Aceh, Indonesia. The chemicals used were sulfuric acid (Merk Emsure® Germany), NaOH (Merk Emsure® Germany), H_2O_2 35% food-grade, and distilled water.

Procedure

Fiber preparation

The *barangan* banana peduncles were cut into pieces and pressed using a pressing machine to obtain the fiber. The fibers were then dried and ground using a grinder GM-400S1 at a speed of 31000 rpm and sieved using a 40 mesh sieve.

Cellulose extraction

The alkalization process was done by a microwave (Samsung ME731K) with a 1 M NaOH solution (1:15 w/v) at 450 Watt with a temperature of around 90 °C for 1 h. The fiber was then washed to a neutral pH and dried at 60 °C using a hot air sterilizer oven (model: YCO-010, Taiwan). Following the polymerization process, the bleaching process was conducted for one hour using 35% H_2O_2 with a fiber-to-solution ratio of 1:15 (w/v) at 180 W microwave power and a temperature range of 60–65 °C. This process was to remove compounds other than cellulose [41].

Isolation of nanocrystalline cellulose

The isolation of NCCs was conducted by sulfuric acid hydrolysis with the concentrations of 1, 2, and 3 M with a ratio of a sulfuric acid solution of 1:15 (w/v). This process was done by a microwave (Samsung ME731K) at 100 W for 0.5 and 1.5 h, as presented in Fig. 1. Once the hydrolysis process was completed, the sample was washed using distilled water to reach a neutral pH. Next, the samples were centrifuged using a centrifuge (CMC supplied by Phillip Harris INT) at 11000 rpm for 30 min. The water was changed twice, followed by the sonification process using ultrasonics (Branson model 5510, USA) with a frequency of 40 kHz for 4 h. It was centrifuged for 30 min and dried using a hot air sterilizer oven (model YCO-010, Taiwan) at 60 °C to a maximum moisture content of 12%. Later, it was ground and sieved using a 500 mesh sieve ASTM No: 11. The design of the NCCs isolation treatment is shown in Table 1. The analysis was then conducted for the yield and the characterization of NCCs properties, namely, morphological properties, functional groups, crystallinity properties, heat resistance, particle size, and color.

Characterization of nanocrystalline cellulose

Yield. The yield was calculated as a percentage (%) of the initial weight after hydrolysis. The samples obtained after the treatment were dried and compared to the initial weight. Yield is determined using Eq. (1) [42].

$$\text{Yield}(\%) = \frac{\text{Ma}}{\text{Mi}} \quad (1)$$

The final (Ma) and initial sample weights (Mi) were measured to calculate the yield.

Table 1. Design of NCCs isolation treatment

Samples	Treatment
SA-1	Sulfuric acid 1 M/0.5 h
SA-2	Sulfuric acid 1 M/1.5 h
SU-1	Sulfuric acid 2 M/0.5 h
SU-2	Sulfuric acid 2 M/1.5 h
SM-1	Sulfuric acid 3 M/0.5 h
SM-2	Sulfuric acid 3 M/1.5 h

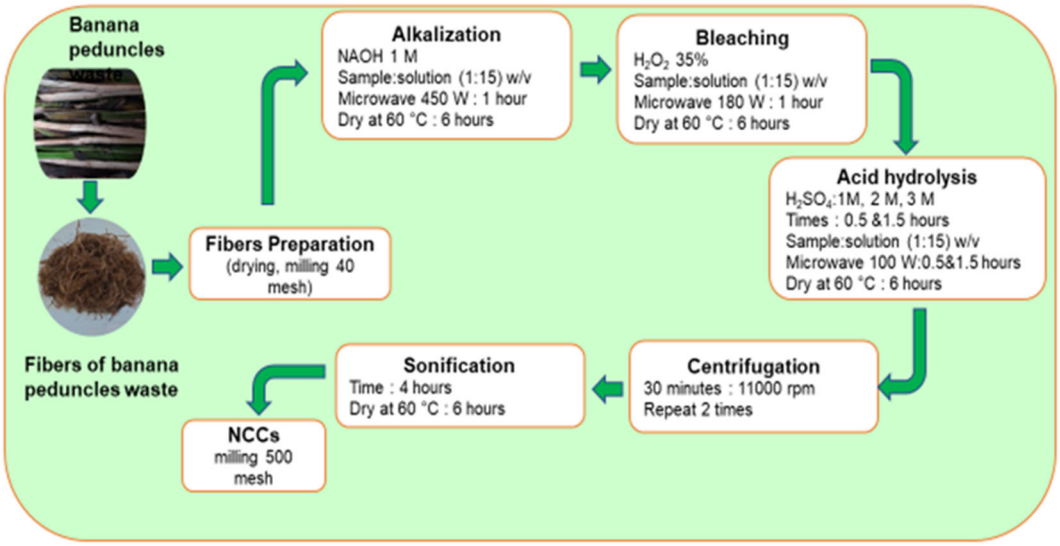

Fig 1. Schematic diagram of the NCCs insulating process

Functional groups. Fourier transform infrared spectroscopy (FTIR, Shimadzu, Japan) was used to determine the functional groups of NCCs products. The NCCs sample was dried in an oven at 60 °C until constant weight to ensure it was free from water content. Then, the NCCs sample was placed on the FTIR panel, and the functional groups were read in the wavenumber of 4000–400 cm^{-1}.

Heat resistance. The heat resistance of gelatin was analyzed using a Thermogravimetric Analyzer (Shimadzu DTG-60, Japan). The sample (10 mg) was put into a platinum pan and then heated to a temperature of 600 °C at a nitrogen atmosphere flow rate of 50 mL/min and a temperature rate of 40 °C/min.

Morphological properties. Morphological studies of samples were done by Scanning Electron Microscopy (SEM, JEOL, JSM-6510LA, Japan) with a resolution of 3.0 nm at 30 kV. To obtain quantitative data on the particle size of NCCs, the SEM images were analyzed using ImageJ software. ImageJ software was used to determine the particle diameter (d) of the NCCs. The particle measurement in the SEM test is based on the sphere's diameter because it cannot be equated with the particle length of the NCCs.

Crystallinity properties. Crystallinity and crystal size were measured using an XRD (Shimadzu-7000, Japan) operated at a voltage of 40 kV and a current of 30 mA, with a scan speed of 2.00 deg/min. The crystallinity index (CI) was calculated based on the deconvolution method, as formulated in Eq. (2).

$$CI = \frac{I_{002} - I_{am}}{I_{002}} \times 100\% \quad (2)$$

where I_{002} is the highest peak intensity for the crystalline region and I_{am} is the minimum peak intensity for the amorphous region. I_{002} represents the crystalline and amorphous regions, while I_{am} only represents the amorphous region of the maximum intensity of the lattice peak diffraction at 22° to 23° and I_{am} is the amorphous part of the material (at the minimum intensity between 18° and 19°) [43-44]. The crystal size was calculated using the Scherrer formula, as given in Eq. (3).

$$t = \frac{K\lambda}{\beta 1/2 \cos\theta} \quad (3)$$

where K (0.91) is the Scherrer constant, λ (1.54060 Å) is the wavelength of the radiation, β1/2 is the full width at half maximum (FWHM) of the diffraction peak in radians (2θ), and θ is the Bragg angle [40].

Particle size analyzer. Particle size distribution analysis was performed using a particle size analyzer (HORIBA Scientific SZ-100, Japan) with a scattering angle of 90°, holding temperature of 25.1 °C, and measurement time of 5.12 sec at a rate of 225 kcps. The average particle diameter size of each sample was taken from the average value of three repetitions.

NCCs powder color test. The color of the NCCs was analyzed using the CIE method. CIE is the most comprehensive L* a* b* color space defined by the International Commission on color illumination (French Commission Internationale de l'eclairage, CIELAB). CIELAB can describe all kinds of colors visible to the human eye. This method is often used for color space references [44]. The NCCs image was then analyzed for color using the MVtec Halcon ver.20 software. The sample object was separated by 15 times erosion treatment to get the RGB value. The resulting RGB (Red, Green, Blue) values were converted to the L* a* b* color space.

■ RESULTS AND DISCUSSION

Yield

Yield is the result of the processing activity. The average yield of fiber from the waste of fresh banana peduncles was 5.4%. The alkalization treatment used 1 M NaOH and 35% H_2O_2 for bleaching. The fiber yield produced in the alkalization process and the bleaching process was 39.5%, with a mass loss of 60.5, and 71%, with a mass loss of 29%, respectively. The more stages in the process, the higher the result because most of the lignin and hemicellulose were removed [45]. Alkalization treatment can remove hemicellulose, reducing weight from 33% to 12%. The alkalization process can reduce the lignin and hemicellulose content and enable the fiber to be easily damaged by the hydrolysis media [35]. Also, H_2O_2 can remove more lignin [46]. Alkalization triggers a color change linked to the different pigmentation of the lignin fraction remaining in

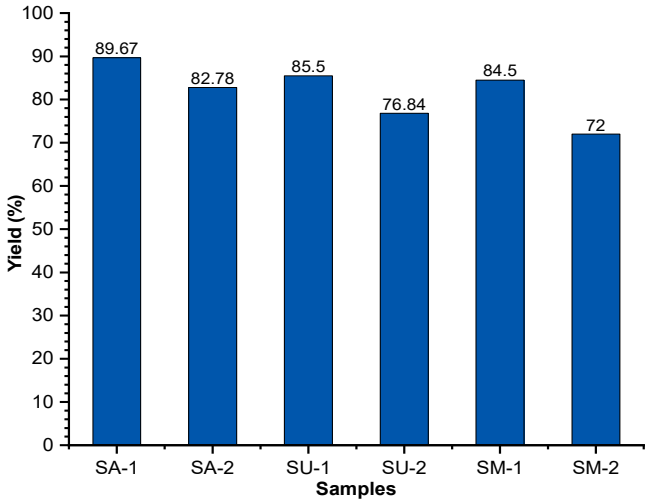

Fig 2. The yield of NCCs isolated from the waste of banana peduncles

the substance [47]. It effectively purifies cellulose fibers, removing non-cellulose components, such as parts of lignin and hemicellulose [13]. The treatment of NaOH solution converts cellulose I to cellulose II with a crystal structure that is much more stable than cellulose I, with stronger hydrophobic interconnections. The hydrolysis yield is shown in Fig. 2.

The yield of NCCs from the treatment variables of different sulfuric acid concentrations and hydrolysis time ranged from 72% to 89.67%, with a mass loss of around 28.00–10.33%. The highest yield was in the treatment of SA-1 (89.67%). Meanwhile, the lowest yield was at the treatment of SM-2 (72%). The yield of NCCs decreased with the increasing sulfuric acid concentration and the hydrolysis time, as shown in Fig. 2. This decrease in yield may be due to the changes in amorphous cellulose or damage to crystalline cellulose [8].

The low yield may result from the gradual disintegration of the amorphous region and degradation of the crystalline moiety during the increasing hydrolysis time. Raja et al. [28] glucose microfibers of cellulose molecules were bonded to form long polymer chains, and the content of lignin and hemicellulose around the cellulose was the main obstacle to hydrolyzing cellulose. Ilyas et al. [8] produce sugar palm cellulose yield in the hydrolysis process using sulfuric acid with a concentration of 60%, which is 82.33%. Seta et al. [6] reported that the yield of NCCs bamboo pulp hydrolyzed using maleic acid was in the range of 2.8% to 24.5%. In this study, treatment with sulfuric acid concentration and hydrolysis time assisted by microwave and ultrasonic energy was able to produce yields ranging from 72% to 86.67%.

Functional Groups of NCCs

Fig. 3 displays the results of the FTIR spectrum of NCCs from *barangan* banana peduncles using the hydrolysis treatment of sulfuric acid concentration and hydrolysis time. It shows three main absorption spectra, the largest indicated at the absorption region around 3200–4000 cm^{-1} was O-H, 2500–3200 cm^{-1} was C-H, and 500–1500 cm^{-1} was C-O. The increasing concentration of sulfuric acid and the hydrolysis time did not affect the absorption and functional groups of NCCs, showing that the NCCs did not contain functional groups of other compounds, such as lignin and hemicellulose. Acid hydrolysis did not show any absorption region for C=C, C–O–C, and $–CH_2$ bonds [48]. The C=C and C–O–C bonds are found in lignin. The absorption region around 1420 cm^{-1} showed a deformed $–CH_2$ bond in cellulose. It showed the crystalline area, where the absorption area increases with the purification process. After hydrolysis, three main absorption regions were found: 3288.08, 1636.43, and 1089.92 cm^{-1}, indicating O–H stretching, O–H deformation, and C–C stretching, respectively. The absorption region that emerged indicates no lignin generated from the acid hydrolysis treatment.

The spectra were identified at the absorption of 3350 cm^{-1} (O–H stretching/intramolecular hydrogen bond stretching for cellulose I), 2900 cm^{-1} (C–H stretching), 1640 cm^{-1} (O–H bending due to adsorbed water), 1510 cm^{-1} (aromatic ring in lignin), 1420 cm^{-1} (due to the scissoring motion of CH_2 in cellulose), 1375 cm^{-1} (C–H bending), 1340 cm^{-1} (O–H in the bending plane), 1311 cm^{-1} (CH_2 wagging), 1250 cm^{-1} (C–O exiting the stretching plane because of the aryl groups in lignin), 1205 cm^{-1} (S=O vibrations, due to the esterification reaction occurred in the hydrolysis), 1159 cm^{-1} (C–C stretching ring), 1109 cm^{-1} (C–O–C glycosidic bond), 1061 cm^{-1} (C–O–C pyranose ring stretching), and 897 cm^{-1} (cellulose glycosidic bonds) [19,50-52]. The vibrational modes of amide I at 1616 cm^{-1}

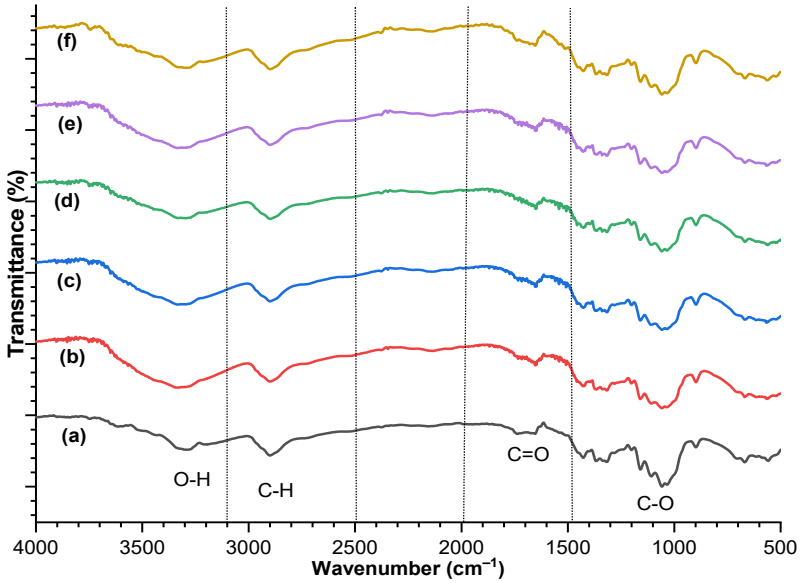

Fig 3. FTIR spectra of NCCs from *barangan* banana peduncles; (a) SA-1; (b) SA-2; (c) SU-1; (d) SU-2; (e) SM-1; and (f) SM-2

and II at 1597 cm^{-1} were observed. The moderate to strong IR absorption band at 1200–970 cm^{-1} was mainly due to the C–C and C–O stretching of the pyranoid ring [49]. The IR spectra of the NCCs showed a typical absorption band for cellulose substances. The signals at 1429, 1163, 1111, and 897 cm^{-1} indicated the NCCs in cellulose Iβ [50]. The absorption bands at around 1430, 1370, and 2900 cm^{-1} indicated the characteristic of the crystalline region in the polymer, and the absorption band at 890 cm^{-1} showed the type of the amorphous region [51]. Hydrolysis with sulfuric acid did not modify the functional groups of cellulose; instead, discontinuities in the glucose ring only [52].

Heat Resistance of NCCs

The TGA method is a rapid test for measuring a material's thermal stability to predict its real-life and long-term stability. The thermal decomposition process occurred in the compound follows first-order kinetics [53]. The results of the thermogravimetric analysis to examine the thermal stability of NCCs from banana peduncles hydrolyzed with 1, 2, and 3 M sulfuric acid for 0.5 and 1.5 h can be seen in Fig. 4. It shows the initial weight loss of the NCCs was in around region 2 with a temperature range of 95.0 to 180.0 °C because volatile compounds and water molecules evaporated. In regions 3 and 4, the NCCs decomposed at a temperature of 275.35 to 409.40 °C.

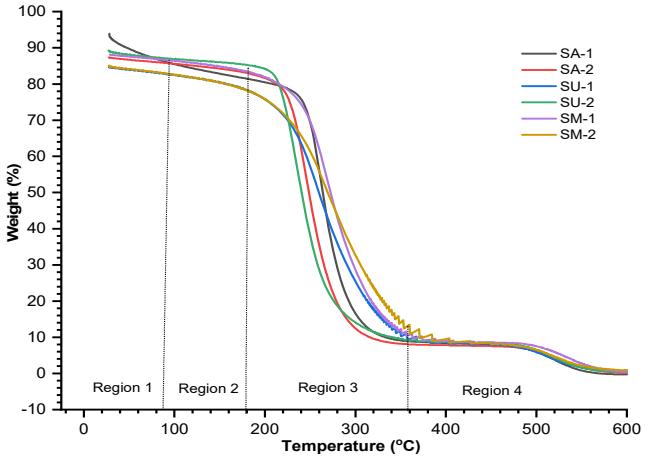

Fig 4. Heat resistance of NCCs from *barangan* banana peduncles

Table 2 shows that the degradation or decomposition of NCCs began to occur in the temperature range of 275.35 to 409.40 °C. The greater the concentration of sulfuric acid, the higher the endset temperature (temperature of degradation). Likewise, the hydrolysis time also showed the difference in the decomposition temperature because of hemicellulose and amorphous cellulose, which were more easily degradable than crystalline cellulose. The wider lignin peak covered

Table 2. Thermal degradation, weight loss, and residue of the NCCs from *barangan* banana peduncles

Samples	Cellulose thermal degradation			Weight loss (%)	Residue at 600 °C (%)
	T_{onset} (°C)	$T_{mid\ point}$ (°C)	T_{endset} (°C)		
SA-1	319.67	348.29	380.83	94.09	5.91
SA-2	340.01	366.69	398.83	87.14	12.86
SU-1	294.10	345.60	405.62	84.10	15.90
SU-2	347.15	373.91	404.08	88.83	11.17
SM-1	314.13	351.22	399.19	87.71	12.29
SM-2	275.35	338.62	409.40	84.00	16.00

the range from 200 to 500 °C, with the maximum at 350 °C. In a nitrogen atmosphere, the main peak appeared at around 360 °C due to the decomposition of α-cellulose [54]. In addition, lignin degradation occurred gradually from 100 to 900 °C, with the disintegration peak occurring after 380 °C. Thus, an additional endothermic peak after 350 °C happened due to the degradation of residual lignin molecules. The presence of foreign material in cellulose samples increased the energy needed for degradation [12]. In the initial temperature region of 70 to 140 °C, the peak endothermic heat energy absorbed was used to evaporate water vapor. Outside of 200 °C, the second and third endotherms were 257.1 and 282.7 °C. This endotherm was related to the decarboxylation and depolymerization of cellulose [13]. The bleaching and alkali processes generated α-cellulose as a crystalline residue. The higher the crystal structure, the higher the degradation temperature [42].

The weight loss due to the treatment of sulfuric acid concentration and hydrolysis time ranged between 84% and 94.09%, with the highest weight loss occurring in the treatment of SA-1 and the lowest in the treatment of SM-2. The treatment of SA, SU, and SM resulted in degradation in the same region, namely region 4. This indicates that the resistance of NCCs to temperature is the same even though the weight loss shows different values. This shows that the resistance characteristics of the NCC samples to temperature are the same. A high weight loss indicates a small residue [13]. The relatively low weight loss indicates a strong cellulose structure to withstand high-temperature conditions. The water loss and the structural hydrophilic nature of the functional groups of each polysaccharide occur between 50 and 100 °C [25].

Hemicellulose loss occurred between 220 and 340 °C, with the main degradation peak around 320 °C. The thermal stability of NCCs with sulfate groups could be improved when the acid sulfate groups were neutralized [39]. Under different conditions, samples of NCCs showed gradual weight loss at around 210 to 378 °C [55].

Morphology of NCCs

Fig. 5 images the morphological microstructure of NCCs from *barangan* banana peduncles treated with sulfuric acid concentrations of 1, 2, and 3 M and hydrolysis times of 0.5 and 1.5 h. Although the sulfuric acid content and hydrolysis time are different, the morphology of the NCCs has the same structure (as displayed in Fig. 5). The size of the resulting NCCs was also the same for all treatments, namely 1 μm. The structure looks like the occurrence of aggregates in the NCCs particles. Wu et al. [38] resulted in the size of the structure of okara nanocellulose (using the method of high-pressure ultrasound or high-pressure homogenization) based on scanning electron microscopy, which was in the range of 2 to 10 μm. Samples of okara nanocellulose also showed the occurrence of aggregation.

Seta et al. [6] convey that the fibers are reduced in size to micro size, and there is a possibility of reaggregation of the fibers of small size. It can be caused by the milling process's activation/interaction of the fiber surface, and the high fiber concentration will increase the friction and shear forces between the fibers. This study resulted in a smaller structure size of NCCs from *barangan* banana peduncles (1 μm) than that produced by Wu et al. [38], which is 2 to 10 μm. The particle diameter (d) of

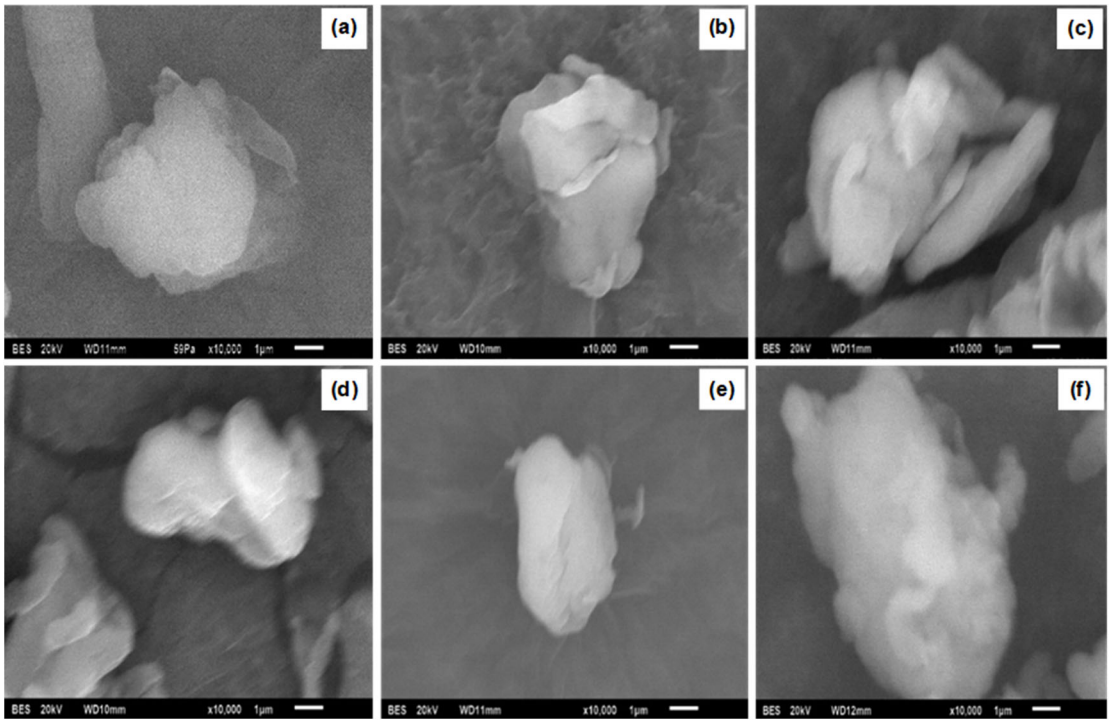

Fig 5. SEM image of NCCs banana peduncles; (a) SA-1, (b) SA-2, (c) SU-1, (d) SU-2, (e) SM-1, and (f) SM-2

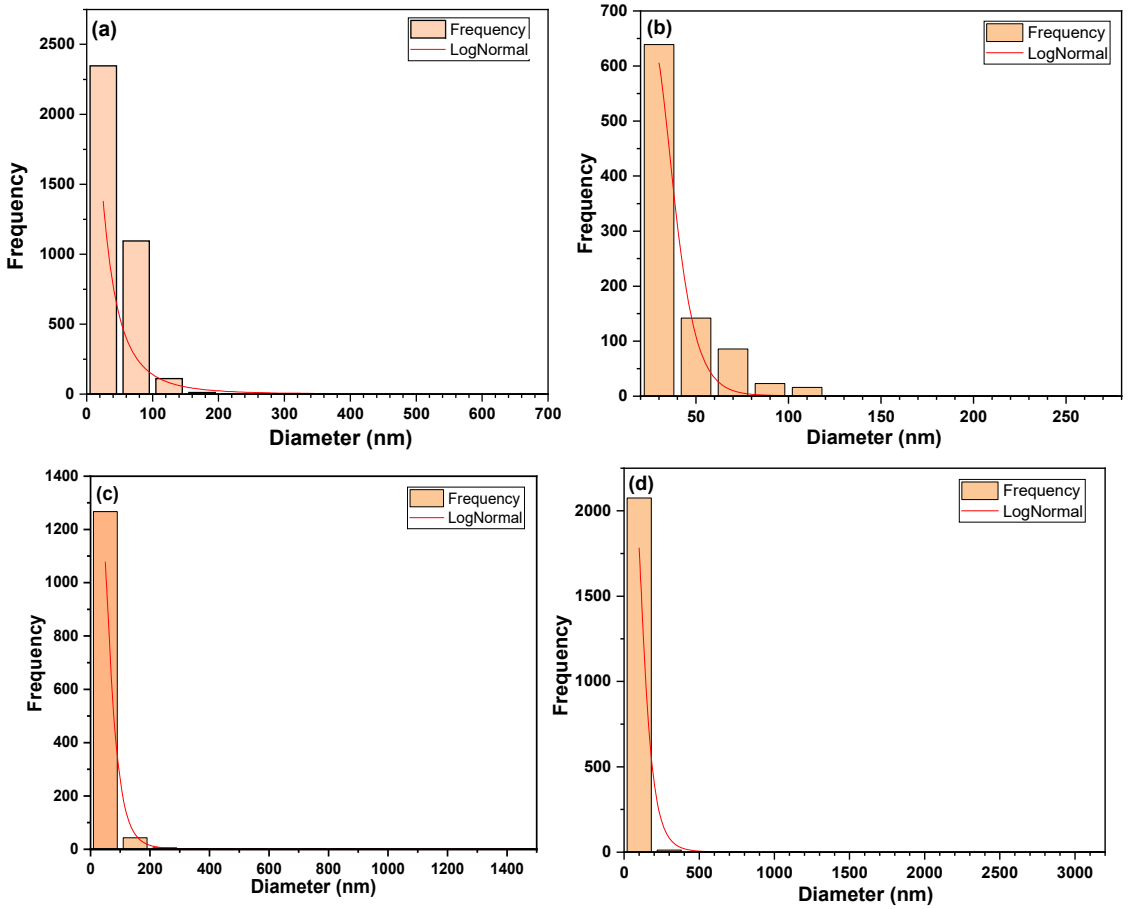

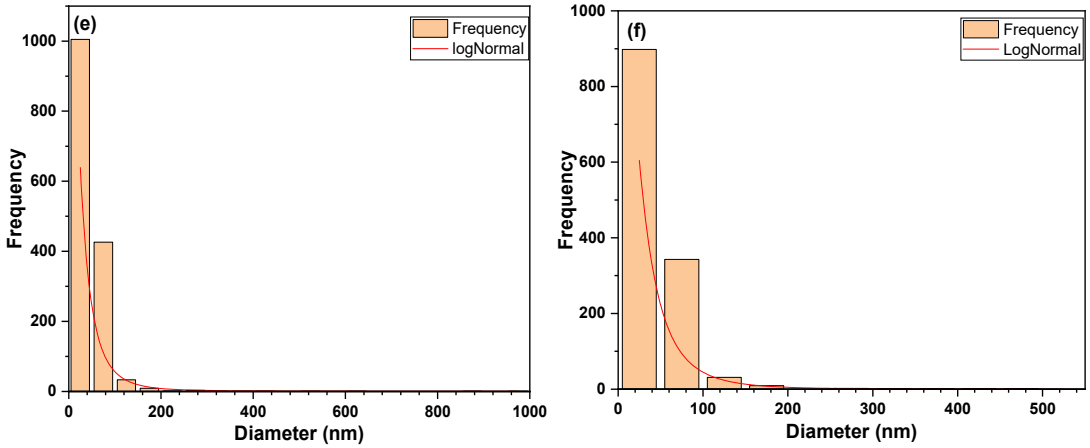

Fig 6. Histogram distribution of NCCs particles from SEM images; (a) SA-1, (b) SA-2, (c) SU-1, (d) SU-2, (e) SM-1, and (f) SM-2

the NCC samples from the SEM test results can be quantitatively analyzed using ImageJ software. Regarding the SEM image analysis using ImageJ software, the histogram of the NCCs particle distribution can be seen in Fig. 6, and the diameter of particles can be seen in Table 3. The particle diameter analysis using ImageJ software of NCCs for all treatments of sulfuric acid concentration and hydrolysis time ranged from 25 to 100 nm.

Crystallinity Properties of NCCs

Enhanced crystallinity can increase the heat resistance and thermal stability of a material. A further decrease in the degradation temperature of NCCs may correlate with sulfate groups into crystalline cellulose during the hydrolysis of sulfuric acid [56]. Fig. 7 presents the X-ray diffraction pattern of the NCCs from banana peduncles. The diffraction peaks at 2θ for 1, 2, and 3 M sulfuric acids with the hydrolysis times of 0.5 and 1.5 h ranged from 22.19°–22.41°. All diffraction patterns for all treatments are at the highest peak at 2θ above 22° [9,57-58]. The observed peaks in the XRD pattern of cellulose and NCCs at 2θ of 14.5° and 15.5° correspond to I_{am} planes. The peak of 2θ = 22.5° corresponds to the I_{002} crystallographic plane, indicating that cellulose and nanocellulose had amorphous and crystalline regions and showed the crystal structure of cellulose I.

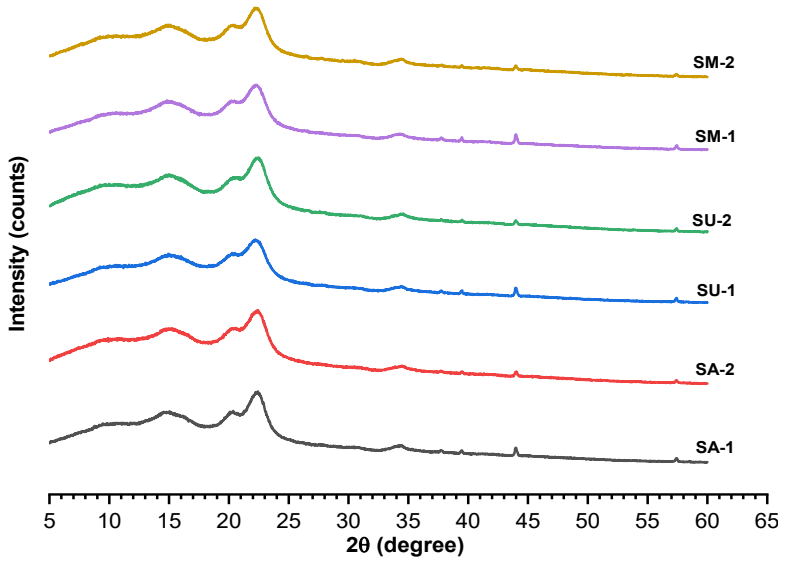

Fig 7. X-ray diffraction pattern of NCCs from *barangan* banana peduncles

Table 3. Crystallinity index (CI), crystal size, and diameter particle (SEM image) of NCCs

Samples	2θ (am)	2θ (002)	CI	Crystal size	ImageJ (SEM image)	
	(°)	(°)	(%)	(nm)	d (nm)	R^2
SA-1	14.82	22.23	57.33	34.38	25	0.72
SA-2	14.75	22.41	56.69	22.35	30	0.98
SU-1	15.04	22.31	54.96	27.94	50	0.98
SU-2	14.98	22.19	55.38	36.28	100	0.98
SM-1	14.99	22.33	53.99	27.43	25	0.78
SM-2	14.81	22.35	55.19	23.67	25	0.81

In the XRD pattern, the absorption peaks tend to have a narrower peak width and higher peaks with high crystallinity. For materials with low crystallinity, the absorption peaks show a wider peak width and lower peak height [59]. Sharp diffraction peaks and flat dispersion curves simultaneously emerge since the composition of the crystalline and amorphous phases of the polymeric material. Structural changes can be due to forces that occur during mechanical processes. The shearing force by a high-pressure homogenizer can remove amorphous cellulose, increasing crystallinity [57]. Ultrasonication hydrolyzes the amorphous regions of cellulose and some parts of the broken cellulose fragments to produce oligo and monosaccharides [30]. Table 3 shows the crystallinity index (CI) of NCCs from the treatment of sulfuric acid concentration and hydrolysis time, ranging from 53.99% to 57.33%. The highest CI value was obtained in the treatment of SA-1 (57.33%), while the lowest CI value was in the treatment of SM-1 (53.99%). The crystal size of NCCs was between 22.35 and 36.28 nm, with the largest size being in the treatment of SU-2 (36.28 nm) and the smallest in the treatment of SA-2 (22.35 nm). Hydrolysis at lower concentrations of sulfuric acid (16% and 40% by weight) reduced the amorphous component of the initial pulp. However, the conditions are insufficient to resynchronize the crystals structurally or reduce the crystal size [58,60].

In addition, the intense cavitation force by ultrasound can remove the amorphous zone and decrease the crystalline zone, ultimately decreasing the crystallinity index [61]. The stronger the strain, the wider the diffraction peaks, increasing the microstrain lattice and decreasing the crystal size [62]. This study resulted in the crystal size of NCCs based on the results of the crystallinity test and the particle diameter of the NCCs based on the results of the SEM image test using ImageJ software, which was in the 100 nm range.

The Particle Size of NCCs

Particle size analysis is an analysis of the average particle size distribution in a liquid. Fig. 8 shows the average particle size distribution of NCCs treated with sulfuric acid concentrations of 1, 2, and 3 M and hydrolysis times of 0.5 and 1.5 h (Table 4). The particle sizes of NCCs ranged from 250.9 to 4214.6 nm. The most petite particle sizes, 250.9, 257.9, and 259.2 nm, were obtained at concentrations of 1, 2, and 3 M sulfuric acid, respectively, with a hydrolysis duration of 1.5 h. The smaller the particle size of the NCCs produced, the higher the sulfuric acid concentration. Similarly, the longer the hydrolysis period, the smaller the particle size of the formed NCCs. The criteria for determining particle size and distribution depend on various factors, including sample structure, acid concentration, and hydrolysis time. On the other hand, the particle size distribution depends on the degree of aggregation [63]. Dimas et al. [64] reported that the average size of NCCs hydrolyzed with 6, 8, and 10 M HCl were 8334, 3024, and 2086 nm, respectively, as measured by PSA.

Table 4. Particle size distribution of NCCs *barangan* banana peduncles

Sample	Particle size (nm)	PI
SA-1	4214.6	1.025
SA-2	250.9	0.808
SU-1	4157.3	1.062
SU-2	257.9	0.908
SM-1	3267.5	0.965
SM-2	259.2	0.902

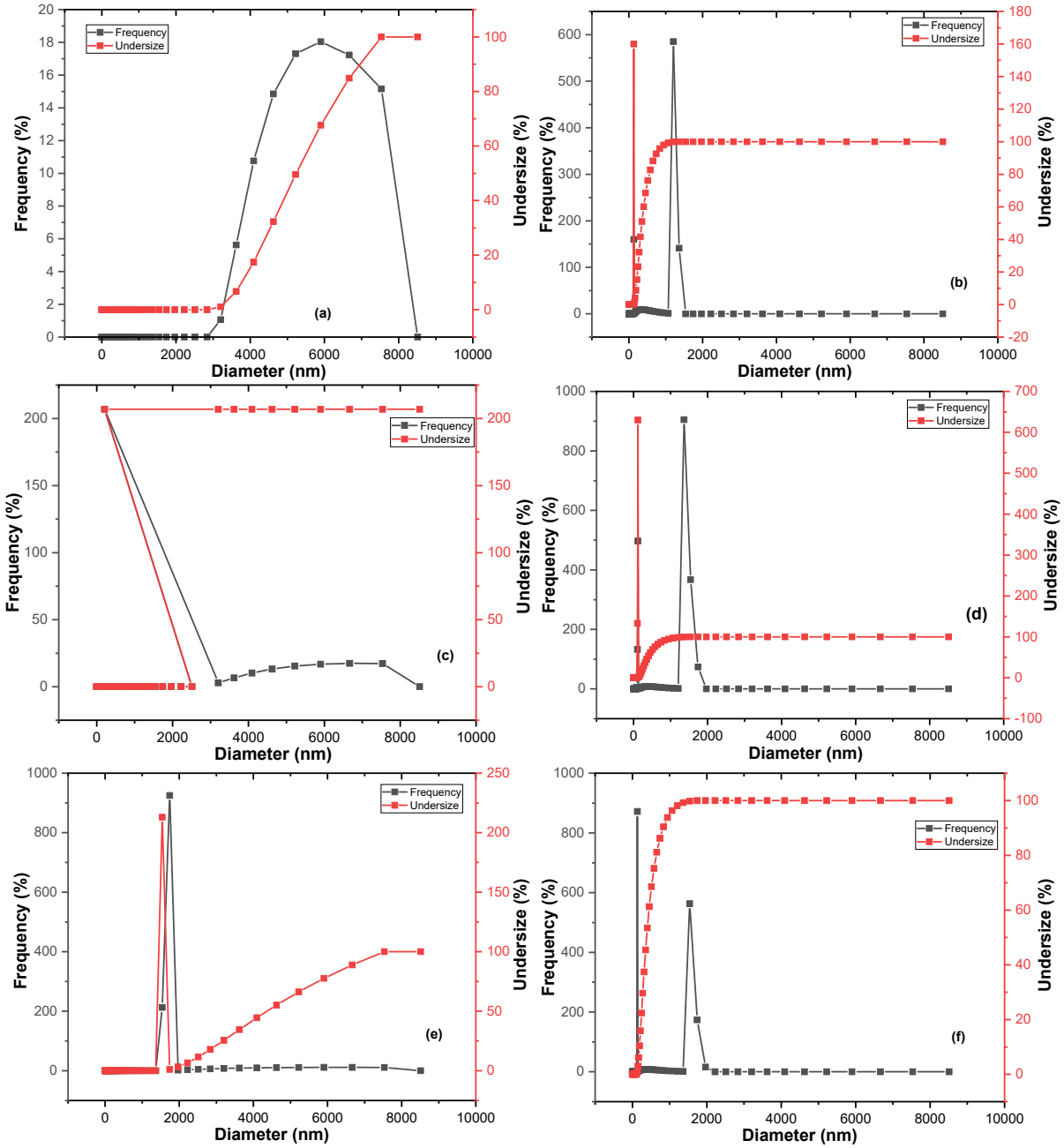

Fig 8. Particle size analyzer of NCCs; (a) SA-1, (b) SA-2, (c) SU-1, (d) SU-2, (e) SM-1, and (f) SM-2

It indicates that NCCs dropped as the concentration of hydrochloric acid increased. After the long fiber amorphous areas were hydrolyzed by acid disintegration to form shorter NCCs particles, the size of the NCCs was reduced. Agglomerates can cause dynamic light scattering, and PSA cannot precisely measure the particle size of single NCCs. In this study, there was a large agglomeration marked by a significant PI (polydispersity index) value above 0.5. The research of Wu et al. [38] produced a particle size of okara nanocellulose (using the method of high-pressure ultrasound or high-pressure homogenization) based on the PSA test, which was in the range of 233–2430 nm with PI values ranging from 0.22 to 0.91.

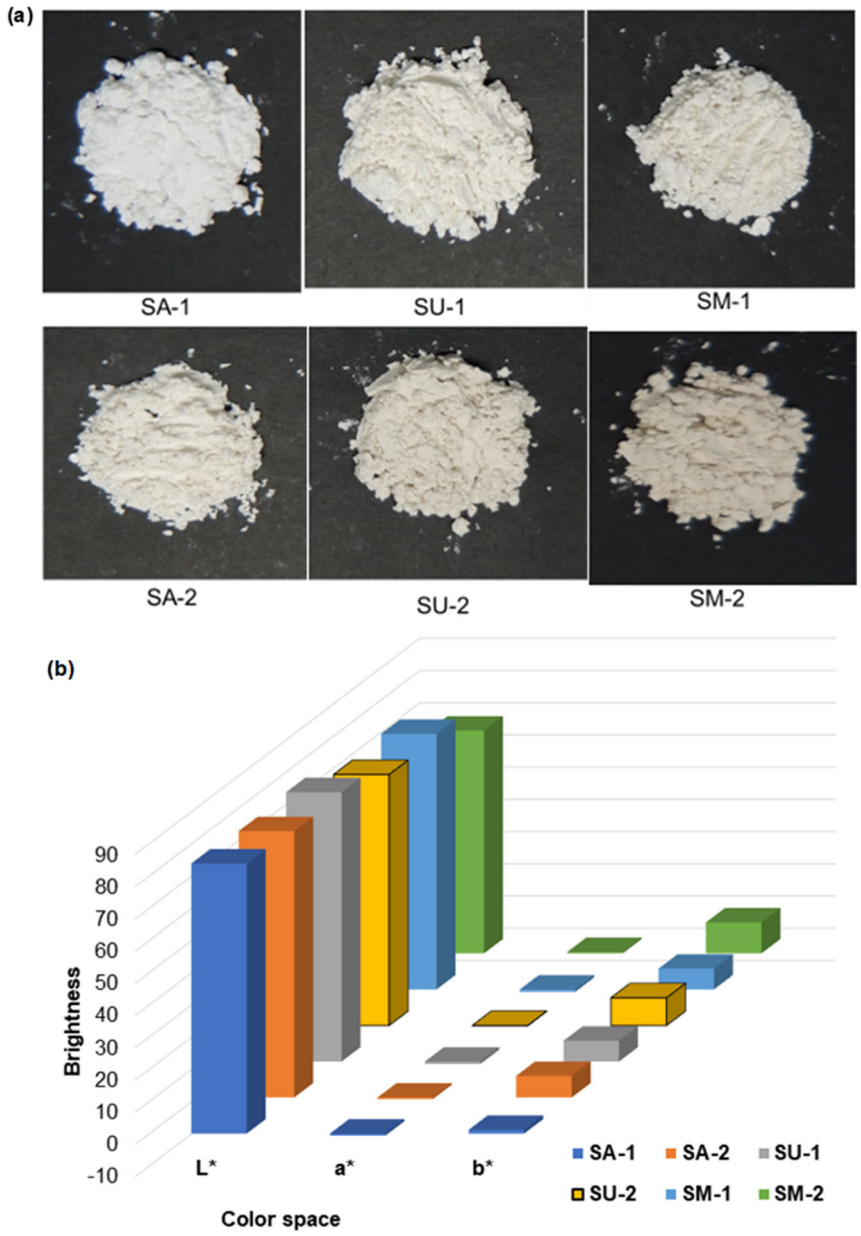

Fig 9. (a) NCCs powder from banana peduncles and (b) CIELAB color space L*a*b* NCCs powder of acid hydrolysis effect

Color of NCCs Powder

Fig. 9(b) describes the brightness of NCCs powder. The L* value is the brightness value; the higher the L*, the brighter the NCCs powder. The L* values range from 69.14 to 83.81. The highest L* brightness value was found in the treatment of SA-1 (83.81). The lowest was in the treatment of SM-2 (69.14). In contrast, the higher the sulfuric acid concentration and hydrolysis time, the higher the a* and b* values. The higher the L* value, the lighter (whiter) the color of the NCCs. Brightness is denoted by L*, ranging from L* = 0 (black) to 100 (white) [65].

The higher the concentration of sulfuric acid and the hydrolysis time, the darker the color of the NCCs powder, as shown in Fig. 9(a). The expected color of the NCCs powder is bright, and thus the best color of NCCs powder was the one that resulted from the treatment of SA-1. The cellulose content in the fiber influences the

fiber absorption of color, resulting in differences in color absorption in each fiber [5]. The increasing amount of polymer will increase light diffusion [65]. Good light reflection is the one directed at the surface of an object. If the surface of an object reflects light in all directions, it will be blunt. The microwave effect is through ionic conduction, which is resistance heating [66]. The collision between the dye molecules and fiber particles depends on the acceleration of the particles through the dye solution.

■ CONCLUSION

Treatment of sulfuric acid concentration and time of hydrolysis assisted by microwave energy resulted in different yields of NCCs. The yield of NCCs decreased with increasing sulfuric acid concentration and hydrolysis time. FTIR test results showed that the concentration of sulfuric acid and hydrolysis time produced NCCs with the same functional groups in the same absorption spectrum zone. TGA test results showed that the decomposition of NCCs occurred at a temperature of 275.35–409.40 °C, with a weight loss ranging from 84% to 94.09%. In addition, the XRD test results revealed that all diffraction patterns for all treatments were at the highest peak of 2θ above 22°, with index crystallinity values ranging from 53.99% to 57.33% and crystal sizes ranging from 22.35 to 36.28 nm. The brightest NCCs powder was obtained from the treatment of 1 M sulfuric acid and 0.5 h of hydrolysis time.

■ ACKNOWLEDGMENTS

This research was supported by Universitas Syiah Kuala, Aceh, Indonesia, through the Institute for Research and Community Service (LPPM) under the Lecturer Research Program [241/UN11.2.1/PT.01.03/PNBP/2021].

■ AUTHOR CONTRIBUTIONS

Ratna**:** Writing, methodology-data analysis, original draft, conceptualization & investigation. Sri Aprilia: Supervision, writing-methodology, review-editing, conceptualization & investigation. Nasrul Arahman: Supervision, review-editing & conceptualization. Agus Arip Munawar: Supervision & review. All authors agreed to the final version of this manuscript.

■ REFERENCES

[1] Adsal, K.A., Üçtuğ, F.G., and Arikan, O.A., 2020, Environmental life cycle assessment of utilizing stem waste for banana production in greenhouses in Turkey, *Sustainable Prod. Consumption*, 22, 110–125.

[2] Padam, B.S., Tin, H.S., Chye, F.Y., and Abdullah, M.I., 2014, Banana by-products: an under-utilized renewable food biomass with great potential, *J. Food Sci. Technol.*, 51 (12), 3527–3545.

[3] Gumisiriza, R., Hawumba, J.F., Okure, M., and Hensel, O., 2017, Biomass waste-to-energy valorisation technologies: A review case for banana processing in Uganda, *Biotechnol. Biofuels*, 10 (1), 11.

[4] Ahmad, T., and Danish, M., 2018, Prospects of banana waste utilization in wastewater treatment: A review, *J. Environ. Manage.*, 206, 330–348.

[5] Nur, C., and Djati, I.D., 2018, Studi daya serap warna serat tandan pisang dengan pembanding serat abaka dan serat sabut kelapa, *Arena Tekstil*, 33 (1), 19–28.

[6] Seta, F.T., An, X., Liu, L., Zhang, H., Yang, J., Zhang, W., Nie, S., Yao, S., Cao, H., Xu, Q., Bu, Y., and Liu, H., 2020, Preparation and characterization of high yield cellulose nanocrystals (CNC) derived from ball mill pretreatment and maleic acid hydrolysis, *Carbohydr. Polym.*, 234, 115942.

[7] Chen, Q., Xiong, J., Chen, G., and Tan, T., 2020, Preparation and characterization of highly transparent hydrophobic nanocellulose film using corn husks as main material, *Int. J. Biol. Macromol.*, 158, 781–789.

[8] Ilyas, R.A., Sapuan, S.M., Atikah, M.S.N., Asyraf, M.R.M., Ayu Rafiqah, S., Aisyah, H.A., Mohd Nurazzi, N., and Norrrahim, M.N.F., 2021, Effect of hydrolysis time on the morphological, physical, chemical, and thermal behavior of sugar palm nanocrystalline cellulose (*Arenga pinnata* (Wurmb.) Merr), *Text. Res. J.*, 91 (1-2), 152–167.

[9] Ng, L.Y., Wong, T.J., Ng, C.Y., and Amelia, C.K.M., 2021, A review on cellulose nanocrystals production and characterization methods from *Elaeis guineensis* empty fruit bunches, *Arabian J. Chem.*, 14 (9), 103339.

[10] Abdul Khalil, H.P.S., Davoudpour, Y., Saurabh, C.K., Hossain, M.S., Adnan, A.S., Dungani, R., Paridah, M.T., Islam Sarker, M.Z., Fazita, M.R.N., Syakir, M.I., and Haafiz, M.K.M., 2016, A review on nanocellulosic fibres as new material for sustainable packaging: Process and applications, *Renewable Sustainable Energy Rev.*, 64, 823–836.

[11] Flores-Velázquez, V., Córdova-Pérez, G.E., Silahua-Pavón, A.A., Torres-Torres, J.G., Sierra, U., Fernández, S., Godavarthi, S., Ortiz-Chi, F., and Espinosa-González, C.G., 2020, Cellulose obtained from banana plant waste for catalytic production of 5-HMF: Effect of grinding on the cellulose properties, *Fuel*, 265, 116857.

[12] Harini, K., and Chandra Mohan, C., 2020, Isolation and characterization of micro and nanocrystalline cellulose fibers from the walnut shell, corncob and sugarcane bagasse, *Int. J. Biol. Macromol.*, 163, 1375–1383.

[13] Kian, L.K., Saba, N., Jawaid, M., Alothman, O.Y., and Fouad, H., 2020, Properties and characteristics of nanocrystalline cellulose isolated from olive fiber, *Carbohydr. Polym.*, 241, 116423.

[14] Camacho, M., Ureña, Y.R.C., Lopretti, M., Carballo, L.B., Moreno, G., Alfaro, B., and Vega Baudrit, J.R., 2017, Synthesis and characterization of nanocrystalline cellulose derived from Pineapple peel residues, *J. Renewable Mater.*, 5 (5), 271–279.

[15] Xu, Y., Atrens, A., and Stokes, J.R., 2020, A review of nanocrystalline cellulose suspensions: Rheology, liquid crystal ordering and colloidal phase behaviour, *Adv. Colloid Interface Sci.*, 275, 102076.

[16] Ghorbani, M., and Roshangar, L., 2021, Construction of collagen/nanocrystalline cellulose based-hydrogel scaffolds: Synthesis, characterization, and mechanical properties evaluation, *Int. J. Polym. Mater. Polym. Biomater.*, 70 (2), 142–148.

[17] Qi, W., Li, T., Zhang, Z., and Wu, T., 2021, Preparation and characterization of oleogel-in-water pickering emulsions stabilized by cellulose nanocrystals, *Food Hydrocolloids*, 110, 106206.

[18] Doh, H., Lee, M.H., and Whiteside, W.S., 2020, Physicochemical characteristics of cellulose nanocrystals isolated from seaweed biomass, *Food Hydrocolloids*, 102, 105542.

[19] Ditzel, F.I., Prestes, E., Carvalho, B.M., Demiate, I.M., and Pinheiro, L.A., 2017, Nanocrystalline cellulose extracted from pine wood and corncob, *Carbohydr. Polym.*, 157, 1577–1585.

[20] Shao, X., Wang, J., Liu, Z., Hu, N., Liu, M., and Xu, Y., 2020, Preparation and characterization of porous microcrystalline cellulose from corncob, *Ind. Crops Prod.*, 151, 112457.

[21] Supian, M.A.F., Amin, K.N.M., Jamari, S.S., and Mohamad, S., 2020, Production of cellulose nanofiber (CNF) from empty fruit bunch (EFB) via mechanical method, *J. Environ. Chem. Eng.*, 8 (1), 103024.

[22] Foo, M.L., Ooi, C.W., Tan, K.W., and Chew, I.M.L., 2020, A step closer to sustainable industrial production: Tailor the properties of nanocrystalline cellulose from oil palm empty fruit bunch, *J. Environ. Chem. Eng.*, 8 (5), 104058.

[23] Kusmono, K., Listyanda, R.F., Wildan, M.W., and Ilman, M.N., 2020, Preparation and characterization of cellulose nanocrystal extracted from ramie fibers by sulfuric acid hydrolysis, *Heliyon*, 6 (11), e05486.

[24] Jiang, Q., Xing, X., Jing, Y., and Han, Y., 2020, Preparation of cellulose nanocrystals based on waste paper via different systems, *Int. J. Biol. Macromol.*, 149, 1318–1322.

[25] Plengnok, U., and Jarukumjorn, K., 2020, Preparation and characterization of nanocellulose from sugarcane bagasse, *Biointerface Res. Appl. Chem.*, 10 (3), 5675–5678.

[26] Mocktar, N.A., Abdul Razab, M.K.A., Mohamed Noor, A., and Abdullah, N.H., 2020, Preparation and characterization of kenaf and oil palm nanocellulose by acid hydrolysis method, *Mater. Sci. Forum*, 1010, 495–500.

[27] Haldar, D., and Purkait, M.K., 2020, Micro and nanocrystalline cellulose derivatives of lignocellulosic biomass: A review on synthesis, applications and advancements, *Carbohydr. Polym.*, 250, 116937.

[28] Raja, P.M., Rangkuti, I.U.P., Hendra Ginting, M., Giyanto, G., and Siregar, W.F., 2021, Preparation

and characterization of cellulose microcrystalline made from palm oil midrib, *IOP Conf. Ser.: Earth Environ. Sci.*, 819, 012002.

[29] Mohd Ishak, N.A., Khalil, I., Abdullah, F.Z., and Muhd Julkapli, N., 2020, A correlation on ultrasonication with nanocrystalline cellulose characteristics, *Carbohydr. Polym.*, 246, 116553.

[30] Abdul Khalil, H.P.S., Davoudpour, Y., Sri Aprilia, N.A., Mustapha, A., Hossain, M.S., Islam, M.N., and Dungani, R., 2014, "Nanocellulose-Based Polymer Nanocomposite: Isolation, Characterization and Applications" in *Nanocellulose Polymer Nanocomposites*, Eds. Thakur, V.K., Scrivener Publishing LLC, Wiley, Massachusetts, 273–309.

[31] Villalobos, K., Rojas, H., González-Paz, R., Granados, D.B., González-Masís, J., Baudrit, J.V., and Corrales-Ureña, Y.R., 2017, Production of starch films using propolis nanoparticles as novel bioplasticizer, *J. Renewable Mater.*, 5 (3-4), 189–198.

[32] Tiwari, G., Sharma, A., Kumar, A., and Sharma, S., 2019, Assessment of microwave-assisted alkali pretreatment for the production of sugars from banana fruit peel waste, *Biofuels*, 10 (1), 3–10.

[33] Abdul Khalil, H.P.S., Chong, E.W.N., Owolabi, F.A.T., Asniza, M., Tye, Y.Y., Rizal, S., Nurul Fazita, M.R., Mohamad Haafiz, M.K., Nurmiati, Z., and Paridah, M.T., 2019, Enhancement of basic properties of polysaccharide-based composites with organic and inorganic fillers: A review, *J. Appl. Polym. Sci.*, 136, 47251.

[34] Chavan, R.R., and Hosamani, K.M., 2018, Microwave-assisted synthesis, computational studies and antibacterial/anti-inflammatory activities of compounds based on coumarin-pyrazole hybrid, *R. Soc. Open Sci.*, 5 (5), 172435.

[35] Chowdhury, Z.Z., and Abd Hamid, S.B., 2016, Preparation and characterization of nanocrystalline cellulose using ultrasonication combined with a microwave-assisted pretreatment process, *BioResources*, 11 (2), 3397–3415.

[36] Ilyas, R.A., Sapuan, S.M., Sanyang, M.L., Ishak, M.R., and Zainuddin, E.S., 2018, Nanocrystalline cellulose as reinforcement for polymeric matrix nanocomposites and its potential applications: A review, *Curr. Anal. Chem.*, 14 (3), 203–225.

[37] Silva-Castro, I., Martín-Ramos, P., Matei, P.M., Fernandes-Correa, M., Hernández-Navarro, S., and Martín-Gil, J., 2017, "Eco-Friendly Nanocomposites of Chitosan with Natural Extracts, Antimicrobial Agents, and Nanometals" in *Handbook of Composites from Renewable Materials*, Eds. Thakur, V.K., Thakur, M.K., and Kessler, M.R., Scrivener Publishing LLC, Wiley, Massachusetts, 35–60.

[38] Wu, C., McClements, D.J., He, M., Zheng, L., Tian, T., Teng, F., and Li, Y., 2021, Preparation and characterization of okara nanocellulose fabricated using sonication or high-pressure homogenization treatments, *Carbohydr. Polym.*, 255, 117364.

[39] Wang, H., Xie, H., Du, H., Wang, X., Liu, W., Duan, Y., Zhang, X., Sun, L., Zhang, X., and Si, C., 2020, Highly efficient preparation of functional and thermostable cellulose nanocrystals via H_2SO_4 intensified acetic acid hydrolysis, *Carbohydr. Polym.*, 239, 116233.

[40] Rahmawati, C., Aprilia, S., Saidi, T., Aulia, T.B., and Ahmad, I., 2021, Preparation and characterization of cellulose nanocrystals from *Typha* sp. as a reinforcing agent, *J. Nat. Fibers*, 00, 1–14.

[41] Ratna, R., Aprilia, S., Arahman, N., and Munawar, A.A., 2021, Characterization of cellulose nanocrystalline isolated from banana peduncles using acid hydrolysis, *IOP Conf. Ser.: Earth Environ. Sci.*, 922, 012072.

[42] Ilyas, R.A., Sapuan, S.M., and Ishak, M.R., 2018, Isolation and characterization of nanocrystalline cellulose from sugar palm fibres (*Arenga pinnata*), *Carbohydr. Polym.*, 181, 1038–1051.

[43] Gan, P.G., Sam, S.T., Bin Abdullah, M.F., Bin Zulkepli, N.N., and Yeong, Y.F., 2017, Characterization of nanocrystalline cellulose isolated from empty fruit bunch using acid hydrolysis, *Solid State Phenom.*, 264, 9–12.

[44] Rulaningtyas, R., Suksmono, A.B., Mengko, T.L.R., and Putri Saptawati, G.A., 2015, Segmentasi citra berwarna dengan menggunakan metode clustering berbasis patch untuk identifikasi mycobacterium

tuberculosis, *Jurnal Biosains Pascasarjana*, 17 (1), 19–25.

[45] Johar, N., Ahmad, I., and Dufresne, A., 2012, Extraction, preparation and characterization of cellulose fibres and nanocrystals from rice husk, *Ind. Crops Prod.*, 37 (1), 93–99.

[46] Pereira, P.H.F., Waldron, K.W., Wilson, D.R., Cunha, A.P., de Brito, E.S., Rodrigues, T.H.S., Rosa, M.F., and Azeredo, H.M.C., 2017, Wheat straw hemicelluloses added with cellulose nanocrystals and citric acid. Effect on film physical properties, *Carbohydr. Polym.*, 164, 317–324.

[47] Collazo-Bigliardi, S., Ortega-Toro, R., and Chiralt Boix, A., 2018, Isolation and characterisation of microcrystalline cellulose and cellulose nanocrystals from coffee husk and comparative study with rice husk, *Carbohydr. Polym.*, 191, 205–215.

[48] Aditama, A.G., and Ardhyananta, H., 2017, Isolasi selulosa dari serat tandan kosong kelapa sawit untuk nano filler komposit absorpsi suara: Analisis FTIR, *Jurnal Teknik ITS*, 6 (2), 228–231.

[49] Ghazy, M.B., El-Hai, F.A., El-Zawawy, W.K., and Owda, M.E., 2017, Morphology and mechanical properties of nanocrystalline cellulose reinforced chitosan based nanocomposite, *Global J. Chem.*, 3 (1), 125–135.

[50] Leung, A.C.W., Hrapovic, S., Lam, E., Liu, Y., Male, K.B., Mahmoud, K.A., and Luong, J.H.T., 2011, Characteristics and properties of carboxylated cellulose nanocrystals prepared from a novel one-step procedure, *Small*, 7 (3), 302–305.

[51] Alves, L., Medronho, B., Antunes, F.E., Fernández-García, M.P., Ventura, J., Araújo, J.P., Romano, A., and Lindman, B., 2015, Unusual extraction and characterization of nanocrystalline cellulose from cellulose derivatives, *J. Mol. Liq.*, 210, 106–112.

[52] Putri, E., and Gea, S., 2018, Isolasi dan karakterisasi nanokistral selulosa dari tandan sawit (*Elaeis guineensis* Jack), *Elkawnie*, 4, 13–22.

[53] Tritt-Goc, J., Lindner, Ł., Bielejewski, M., Markiewicz, E., and Pankiewicz, R., 2020, Synthesis, thermal properties, conductivity and lifetime of proton conductors based on nanocrystalline cellulose surface-functionalized with triazole and imidazole, *Int. J. Hydrogen Energy*, 45 (24), 13365–13375.

[54] Ludueña, L., Fasce, D., Alvarez, V.A., and Stefani, P.M., 2011, Nanocellulose from rice husk following alkaline treatment to remove silica, *BioResources*, 6 (2), 1440–1453.

[55] Wang, H., Pudukudy, M., Ni, Y., Zhi, Y., Zhang, H., Wang, Z., Jia, Q., and Shan, S., 2020, Synthesis of nanocrystalline cellulose via ammonium persulfate-assisted swelling followed by oxidation and their chiral self-assembly, *Cellulose*, 27 (2), 657–676.

[56] Evans, S.K., Wesley, O.N., Nathan, O., and Moloto, M.J., 2019, Chemically purified cellulose and its nanocrystals from sugarcane baggase: Isolation and characterization, *Heliyon*, 5 (10), e02635.

[57] Sun, Q., Zhao, X., Wang, D., Dong, J., She, D., and Peng, P., 2018, Preparation and characterization of nanocrystalline cellulose/*Eucommia ulmoides* gum nanocomposite film, *Carbohydr. Polym.*, 181, 825–832.

[58] Hamad, W.Y., and Hu, T.Q., 2010, Structure-process-yield interrelations in nanocrystalline cellulose extraction, *Can. J. Chem. Eng.*, 88 (3), 392–402.

[59] Qian, Y., Bian, L., Wang, K., Chia, W.Y., Khoo, K.S., Zhang, C., and Chew, K.W., 2021, Preparation and characterization of curdlan/nanocellulose blended film and its application to chilled meat preservation, *Chemosphere*, 266, 128948.

[60] Liu, Z., Li, X., Xie, W., and Deng, H., 2017, Extraction, isolation and characterization of nanocrystalline cellulose from industrial kelp (*Laminaria japonica*) waste, *Carbohydr. Polym.*, 173, 353–359.

[61] Costa, A.L.R., Gomes, A., Tibolla, H., Menegalli, F.C., and Cunha, R.L., 2018, Cellulose nanofibers from banana peels as a Pickering emulsifier: High-energy emulsification processes, *Carbohydr. Polym.*, 194, 122–131.

[62] Sumadiyasa, M., and Manuaba, I.B.S., 2018, Penentuan ukuran kristal menggunakan formula Scherrer, Williamson-Hull plot, dan ukuran partikel dengan SEM, *Buletin Fisika*, 19, 28–35.

[63] Sri Aprilia, N.A., Davoudpour, Y., Zulqarnain, W., Abdul Khalil, H.P.S., Che Mohamad Hazwan, C.I., Hossain, M.S., Dungani, R., Fizree, H.M., Zaidon, A., and Mohamad Haafiz, M.K., 2016, Physicochemical characterization of microcrystalline cellulose extracted from kenaf bast, *BioResources*, 11, 3875–3889.

[64] Akbar, D.A., Kusmono, K., Wildan, M.W., and Ilman, M.N., 2020, Extraction and characterization of nanocrystalline cellulose (NCC) from ramie fiber by hydrochloric acid hydrolysis, *Key Eng. Mater.*, 867, 109–116.

[65] Maruddin, F., Malaka, R., Baba, S., Amqam, H., Taufik, M., and Sabil, S., 2020, Brightness, elongation and thickness of edible film with caseinate sodium using a type of plasticizer, *IOP Conf. Ser.: Earth Environ. Sci.*, 492, 012043.

[66] Atalla, S.M.M., EL Gamal, N.G., Awad, H.M., and Ali, N.F., 2019, Production of pectin lyase from agricultural wastes by isolated marine *Penicillium expansum* RSW_SEP1 as dye wool fiber, *Heliyon*, 5 (8), e02302.